

# Memory retrieval dynamics and storage capacity of a modular network model of association cortex with featural decomposition

Carlo Fulvi Mari  

23 April 2021

## Abstract

The model network is composed of many modules. Each module represents an assembly of recurrently connected neurons of a neocortical functional unit and operates as a Hebbian autoassociator, storing a number of local configurations of neuronal activity, or *features*, which it can recall upon cue. The global memory *patterns* are made of specific combinations of features sparsely distributed across the modules. Intermodular connections are modelled as a finite-connectivity random graph. Any pair of features in any respective pair of connected modules is allowed to be involved in several memory patterns; the network dynamics is defined in such a way as to overcome the consequent ambiguity of associations. The effects of a hypothetical mechanism of long-range homeostatic synaptic scaling are also investigated.

The dynamical process of cued retrieval almost saturates a natural upper bound while producing negligible spurious activation. The extent of finite-size effects on storage capacity is quantitatively evaluated. In the limit of infinite size, the functional relationship between storage capacity and number of features per module reduces to that which other authors found by methods from equilibrium statistical mechanics, which suggests that the origin of the functional form is fundamentally of combinatorial nature. In contrast with its apparent inevitability at intramodular level, long-range synaptic scaling results to be of minor relevance to both retrieval and storage capacity. A conjecture is posited about how statistical fluctuation of coordination number across the network may underpin spontaneous emergence of semantic hierarchies.

**Keywords:** Modular autoassociator; Network dynamics; Neocortical memory retrieval; Semantic representations; Featural decomposition; Homeostatic synaptic scaling.

## 1 Introduction

Although no definition of anatomical elementary unit of the primate neocortex is universally agreed, there is little doubt that a functional processing unit does exist, though its anatomical boundaries may be not always well defined or very evident. Such functional unit is generally understood to extend vertically through the six cortical layers, to have a base area of the order of  $1\text{mm}^2$ , and to contain a number of neuron in the order of  $10^5$ ; while in some areas it may resemble a column, in other areas it has a more elongated and less regular horizontal section. In the following, a generic unit, called *module*, is defined in terms of its functional properties, refraining from any immediate cytoarchitectonic correspondence.

The neurons inside each module are assumed to be densely interconnected and to also project axons to neurons of other modules. The recurrent connectivity as well as the experimental evidence of reverberating activity have led to the formulation of mathematical models with the aim of understanding, inter alia, how the very numerous modules are organised in terms of architecture of connections and information flow, processing, storage and retrieval. The ultimate objective is, of course, to uncover the mechanistic neuronal underpinning of cognitive processes, which, invariably, involve large scale structures and therefore a multitude of modules. The attention of the present work is especially on the storage and retrieval processes thought to take place in the heteromodal areas of the cortex that are chiefly responsible for semantic memory (Binder et al. 2009). A brief overview of the anatomical and physiological background of the model, as well as its position among the theoretical models already developed, can be found in the Discussion. The focus is now on outlining the present work.

Each module is modelled as an autoassociator that can store a large number of local memories, called *features*. Neurons of any module are assumed to project axons to neurons of other modules, the axonal projections from each module being concentrated onto a relatively small number of other modules, as if following the edges of an underlying dilute random graph. The intermodular, or *long-range*, synapses as well as the intramodular ones are supposed to be Hebbian, so that the large number of modules can function as a multimodular autoassociator. Each global memory *pattern* of the network is hence made of a combination of local features, specific to the pattern, which are represented in a sparse number of modules, the other modules being in a quiescent state. Different patterns involve different combinations of features encoded in different sets of modules, although patterns can share features. The respective states of activation of interconnected modules are positively correlated across the set of memory patterns, which may be related to semantic value. During a putative learning phase, new features may be learned in any module and new Hebbian associations between new or already learned features in different modules may be formed. As any pair of features in respective adjacent modules can be simultaneously involved in more than one pattern, the reactivation of any feature in any module may not determine univocally the features that neighbouring modules should reproduce (*local ambiguity*).

The featural decomposition of memory patterns is biologically and cognitively meaningful. In particular, the sharing of features across patterns may hold semantic value and it can also be argued that it may facilitate important cognitive abilities (e.g., generalisation, analogies and similarities, recognition invariance, statistical inference). A further advantage of functional modularity may concern the economy of memory resources; indeed, if features are sufficiently elementary and, at the same time, not too specific, so to occur in many patterns, they do not need to be learned more than once. All these properties would be hard to achieve in a unimodular, (statistically) homogeneous autoassociator, whereby any new pattern is stored independently.

An accurate balance, possibly by neuromodulation, between the intramodular recurrent processes and the intermodular interactions is needed in order to take advantage of both local featural processes and global cooperation while avoiding to fall into dysfunctional states in which long-range interactions are so strong as to suppress local ones or, conversely, each module is so weakly dependent on the activity of the others that the system may get trapped in a meaningless patchwork of pieces from several memories, known as *memory glass* (O’Kane & Treves 1992, Fulvi Mari & Treves 1998, Fulvi Mari 2000, Fulvi Mari 2004). The dynamics is appropriately defined to overcome these hindrances while being biologically plausible. The network performance is evaluated in terms of cued memory retrieval and storage capacity.

Because features are activated potentially by many patterns during learning, it seems most likely that some homeostatic scaling mechanism intervenes to keep every module in a reasonable working range. In fact, the need for a mechanism of synaptic weight scaling in (unimodular) Hebbian networks has been evident since early theoretical works. Forms of synaptic homeostasis have already been experimentally found and it is not too difficult to envisage what kind of intramodular processes may underpin that function. It seems instead more complicated to devise a mechanism that produce functional scaling of Hebbian synapses between different modules, for they are scattered across a relatively wide range of the cortex and recruited simultaneously less frequently by global activity patterns. As any pair of features in adjacent modules is shared by different patterns much less often during learning than any feature in any module, it is possible that long-range scaling may be dispensable; however, multiple, long-range associations may spread activity at long distances and, therefore, a resolution seems to require quantitative analysis. An answer to such question is attempted in this work by evaluating quantitatively the effect of long-range synaptic scaling on memory storage capacity and cued retrieval.

The choice was made to study out-of-equilibrium dynamics. In general, this allows for delving into the details of activity spread and for not neglecting events with too small a probability rate to happen in a cognitively relevant time-frame, which would instead elude the more common approaches of equilibrium statistical mechanics. As a simple example one may consider the persistence of activity in a wrongly activated module. Commonly adopted stochastic dynamics (irreducible reversible Markov chains) would allow for a positive probability rate of spontaneous decay to quiescence. An equilibrium study, which makes use of the stationary distribution of the stochastic dynamics, would have implicitly let such an event happen an arbitrarily large number of times; however, the typical time-scale for the decay could be much larger than the time-scale of a cognitive window, during which that event may be unlikely to happen. Of course, the present approach has its own drawbacks, first among which the much lesser amenability to mathematical analysis.

The main advancements of the present research with respect to previous results (Fulvi Mari 2004, Fulvi Mari 2000, Fulvi Mari & Treves 1998) are: (1) explicit assignment of numerous local features to each module and actual storage of the relative multiple intermodular featural associations; (2) heuristic and simulation-based estimate of the memory storage capacity of the multimodular network, including quantification of finite-size effects; (3) evaluation of the potential relevance of homeostatic scaling of long-range synapses.

## 2 Model network and dynamics

The dynamical unit is the module of neurons: it is assumed to function as a Hebbian autoassociator that can store and retrieve  $F$  neuronal (local) activity configurations, called *features*. The network is composed of a large number  $M$  of modules, that interact through a net of (quenched) random links, and stores  $P$  global patterns. The dynamics is defined at a coarse-grained modular level, which has foundation on results obtained at the neuronal network level by statistical-mechanical (Renart et al. 1999) and signal-to-noise (Fulvi Mari 2004) analyses of biologically-realistic multimodular models. A table of symbols and acronyms that recur in the following is in Appendix B.

## 2.1 Architecture

The connections between modules are constructed as in a large, extremely dilute undirected simple (i.e., without 1-loops or multiple edges) binomial random graph (Gilbert 1959, Erdős & Rényi 1960, Bollobás 2001): the nodes of the graph represent the modules while the edges represent the connections between modules. The probability for any pair of nodes to be joined by an edge is  $z/M$ , with  $z$  constant, so that the average number of neighbours across modules remains about constant at large, increasing  $M$ . As in standard terminology, modules that are connected to each other are called adjacent and the number of neighbours of any given module is called coordination number of the latter,  $z$  then being called the mean coordination number. It should be noticed that adjacency in graph distance does not reflect geometric closeness and, therefore, any two adjacent nodes may be representing cortical modules that are topographically distant. A highly diluted graph model (edge probability  $\propto \ln(M)/M$ ) could also be used that would guarantee the graph to be connected almost surely in the infinite-size limit; however, with biologically-realistic finite sizes, both graph models are reasonable approximations.

Experimental evidence shows that reciprocal intercolumnar connections in heteromodal cortex are far more frequent than they would be if the connections in the two directions were built independently of each other (Goldman-Rakic 1988, Pucak et al. 1996, Ichinohe et al. 2012). It was therefore decided that a model with reciprocal intermodular connection, albeit still being approximate, is better for multimodular networks than a model with independent directed edges. The best approximation would most likely sit somewhere in between the two extremes, but it would also be less amenable to mathematical and, to a lesser extent, simulation study. Besides, and perhaps more importantly, it seems reasonable that semantically related modules be more likely to interact reciprocally, to the advantage of memory processes.

Figure 1a shows the frequency of nodes in the network as a function of the number of neighbours for three realisations of the graph, with respectively 25,000, 50,000, and 100,000 modules, and the corresponding binomial distribution in dashed histogram. Assuming that a functional column of the neocortical association areas has a horizontal section of about  $1 \text{ mm}^2$ , the simulations described below would then represent 250-1,000  $\text{cm}^2$  of the cortical sheet, equivalent to about 2.5-10% of the total, which seems reasonable (Binder et al. 2009). Deviations of the mean number of neighbours from the expected value predictably decrease in amplitude with larger networks; although being quite small already for the smallest size, they are not negligible in any of them and, together with the randomness of the featural decomposition, they cause visible variability in network properties.

## 2.2 Memory patterns and features

Memory patterns are made of specific combinations of features stored in respective subsets of modules. For each pattern to be stored, the modules that are involved by that pattern are chosen randomly but not independently: on average, any two modules are more likely to be recruited simultaneously if they are adjacent, while they are otherwise recruited independently, in such a way as to keep the network mean activity about the same for all patterns. Summarily,

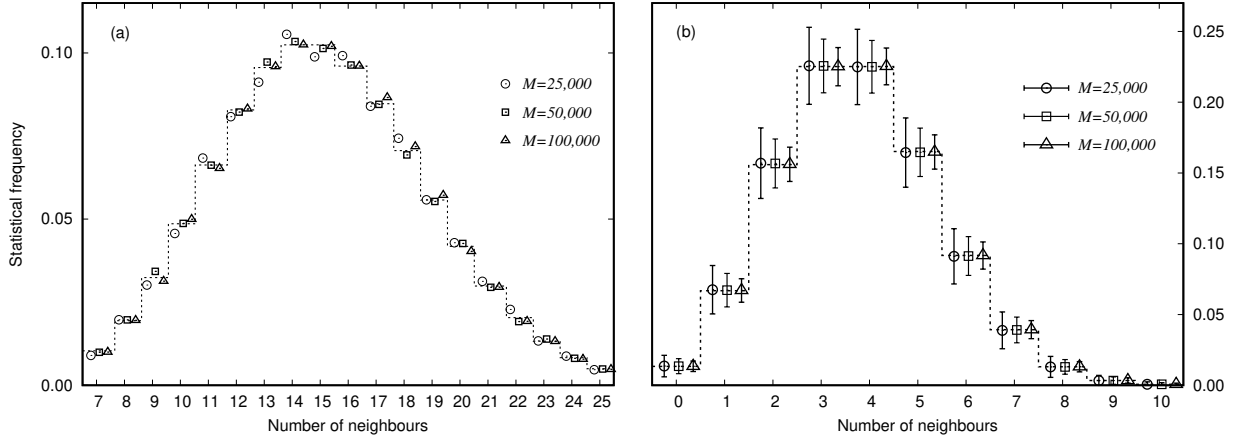


Figure 1: Statistics of model connections and activity patterns: (a) Frequency of nodes as a function of number of neighbours across the graph, the data coming from 3 random graphs of different sizes and the histogram reporting the expected binomial distribution; (b) Frequency of active neighbours of active modules that have in total 15 neighbours, in samples of 20,000 patterns for each of the 3 network sizes (mean and variance stabilise after a few thousands data-points; each error bar is twice as long as the sample standard deviation).

for any modules  $\mathbf{A}$  and  $\mathbf{B}$ , the average marginal probabilities are given by

$$\left\{ \begin{array}{l} \mathbb{P}(\mathbf{A} \text{ active}) = \tau \\ \mathbb{P}(\mathbf{A} \text{ active}, \mathbf{B} \text{ active} \mid \mathbf{A} \leftrightarrow \mathbf{B}) = \tau t_1 \\ \mathbb{P}(\mathbf{A} \text{ quiescent}, \mathbf{B} \text{ active} \mid \mathbf{A} \leftrightarrow \mathbf{B}) = (1 - \tau) t_0 \\ \mathbb{P}(\mathbf{A} \text{ active}, \mathbf{B} \text{ active} \mid \mathbf{A} \not\leftrightarrow \mathbf{B}) = \mathbb{P}(\mathbf{A} \text{ active}) \mathbb{P}(\mathbf{B} \text{ active}) = \tau^2, \end{array} \right. \quad (1)$$

one of the consistency requirements being

$$(1 - \tau) t_0 = (1 - t_1) \tau. \quad (2)$$

This probabilistic scheme was studied, more in detail, mathematically and numerically by Fulvi Mari (2000), where its consistency (and, therefore, physical meaningfulness) was proven to hold in a biologically plausible range of the parameters, and was used by Fulvi Mari & Treves (1998) to suppress memory-glass states. The actual realisation of memory patterns with the correlated statistics is here achieved by numerical implementation of a purposely defined stochastic (heat-bath) process (Fulvi Mari 2000). In the following, the active modules in any memory pattern will be said to constitute the *foreground* (FG) of that pattern, while the quiescent modules will be said to constitute the *background* (BG). Figure 1b shows the distribution of the number of active neighbours of FG modules that have a total of 15 neighbours each, together with the expected histogram.

For each of the  $P$  patterns that recruit a module, a feature is assigned to it, randomly chosen from the  $F$  features stored in that module according to the uniform distribution.

### 2.3 Memory storage and homeostatic synaptic scaling

When the network is made to produce a pattern in the learning stage, associations between features in adjacent modules are stored according to a Hebbian-like rule. If  $\mathbf{A}$  and  $\mathbf{B}$  are adjacent modules and the presented pattern recruits feature  $a$  in  $\mathbf{A}$  and feature  $b$  in  $\mathbf{B}$ , with  $a, b \in [F]$ , an association is created specifically between the two features, formally represented as a unitary increment from null baseline. If another pattern is then presented that recruits the same two features, two possibilities are considered: (1) the weight is incremented by a further unit, or (2) there is no further increment, as the association already exists. In both cases, there is never decrement of the weight, which differs in principle from a covariance rule and does not permit feature-specific inhibition. Case (1) corresponds to the hypothesis according to which synaptic scaling of long-range contacts is not present (nLRSS network), while in case (2) the latter is implemented (LRSS network).

It is assumed that repeated activation of a feature during learning does not engender further Hebbian increments of the synaptic weights between the neurons within the same module, as a consequence of short-range synaptic scaling. Therefore, it is as if any memory feature would only be learned once, while the weights of associations between features in different modules can be repeatedly incremented or not depending on absence or presence of LRSS. Both cases will be taken into account and the respective results then compared.

### 2.4 Network dynamics

If a portion of a stored memory pattern is presented to the quiescent network as a cue, it is a requirement that the dynamics drive the network to retrieve the rest of that memory pattern. Besides, there should be no significant activation of features that do not belong in that pattern. By significant it is meant not only that the fraction of network that is activated be not significantly larger than what would correspond to the exact reactivation of the pattern, but also that any set of wrongly activated features have not significant similarity (i.e., overlap) with any of the other stored patterns. The cue will always be considered as made of complete elementary features rather than individual neuronal firing-rates, in the assumption that any module is capable of quick completion of the local feature when the latter is not fully represented in the cue.

All that follows below can be quite easily formalised mathematically; however, this would unavoidably require the introduction of many symbols, often with multiple indices, which would be cumbersome without being necessary for the understanding or reproducibility of model and results. Therefore, a style of presentation was preferred that be as verbal as possible.

In order to make the description of the dynamical properties of the network more concise, it is useful to first establish some definitions:

**Definition 1** (Association weight). *Let  $\mathbf{A}$  and  $\mathbf{B}$  be any two active adjacent modules, which are reproducing respectively features  $a$  and  $b$ . In the nLRSS network, the **association weight of the pair  $(a, b)$**  is defined as the number of memory patterns that recruit simultaneously those two features. In the LRSS network, the association weight of the pair  $(a, b)$  is equal to 1 if at least one of the memory patterns recruits simultaneously those two features, while it is equal to 0 otherwise. In both cases, the **association weight onto any feature  $a$  in  $\mathbf{A}$**  is equal to the association weight of the pair  $(a, b)$ . If the association weight of  $(a, b)$  is positive, module  $\mathbf{A}$  is said to **support** module  $\mathbf{B}$  (and vice versa).*

**Definition 2** (Compound association weight). *Given any module  $\mathbf{A}$  and its  $n$  active neighbours  $(\mathbf{B}_k)_{k \in [n]}$ , which are respectively reproducing the features  $(b_k)_{k \in [n]}$ , the compound association weight onto any feature  $a$  in  $\mathbf{A}$  is the sum of the association weights of all the pairs  $(a, b_k)_{k \in [n]}$ .*

As an illustrative example, consider the three modules  $\mathbf{A}$ ,  $\mathbf{B}_1$  and  $\mathbf{B}_2$ , with  $\mathbf{B}_1$  and  $\mathbf{B}_2$  being neighbours of  $\mathbf{A}$  (that is,  $\mathbf{B}_1 \leftrightarrow \mathbf{A} \leftrightarrow \mathbf{B}_2$ ) and reproducing, respectively, features  $b_1$  and  $b_2$ . Assume that  $n_1 > 0$  patterns recruit the pair  $(a, b_1)$  and that  $n_2 > 0$  patterns recruit the pair  $(a, b_2)$ . In the nLRSS network, the association weight of the pair  $(a, b_1)$  is  $n_1$ , while that for the pair  $(a, b_2)$  is  $n_2$ ; the compound association weight onto feature  $a$  is then equal to  $n_1 + n_2$ . In the LRSS network, the association weights of the two pairs  $(a, b_1)$  and  $(a, b_2)$  are both equal to 1, and the compound association weight onto feature  $a$  is then equal to 2.

The laws of the dynamics are defined in such a way as to exploit combinatorial properties of memory storage in order to make incorrect activation unlikely enough. They are:

**Law 1** (Oscillations). *During the first stage of cued retrieval, local (featural) dynamical attractors oscillate periodically between a level of high-robustness (HR) and a level of low-robustness (LR); in the second and final stage, robustness is constantly at the lower level. During LR semi-periods, any active feature in any module is stable if the compound association weight onto it is larger than 1; otherwise the module becomes quiescent. During HR semi-periods, any active module will remain active, although it can be forced to switch feature as specified in Law 3.*

**Law 2** (Activity spread). *During HR semi-periods, any quiescent module with active neighbours is driven to retrieve a feature onto which at least one of those reproduced by the neighbours has positive association weight. If different neighbours would drive the module to different featural attractors, the module will reactivate a feature randomly chosen among those onto which the compound association weight has the largest value.*

**Law 3** (Attractor switch). *During HR semi-periods, any active module will stay stable unless the compound association weight onto one of its other features is larger than 1 and than the association weight onto the currently active feature; in such a case, the module will switch to the attractor of a feature randomly chosen among those onto which the compound weight has the largest value.*

Randomness is then present in the model mostly in quenched form: the architecture of the intermodular connections, the involvement of any module in any pattern, and the specific local feature represented by any module recruited by any global pattern. Dynamical randomness is only present in the choice of feature to be activated in any module during retrieval spread if several feature are equally eligible, be it in the activation of a silent module or in attractor switching between features of an already active module. Although such stochastic effect is relatively small and will not be perceptible in the plots from the simulations, it is in play and is visible in the numerical outputs.

### 3 Results

In this Section, properties and behaviour of the network defined above are studied specifically in regards of cued retrieval and stability of memory reactivation against increasing storage load.

### 3.1 Bounds from architecture

The modules that are isolated (i.e., without any neighbour) cannot be affected by the dynamics of the rest of the network and, if activated by the cue, will become silent in the first LR half-wave that follows. A similar argument holds for the modules that belong to trees, that is, connected subsets of nodes with no cycles. If a tree is not cued, it cannot be activated through network dynamics. If a tree is cued, activity will remain during the oscillatory stage and possibly spread within it; what happens in the second stage depends on whether the network has LRSS or not: only in the nLRSS network activity could remain because of pairwise association weights larger than 1, for that is the only way activity can be stable where, as in trees, there are no cycles (Fulvi Mari 2004). Therefore, a general upper bound to retrieval performance that any realistic dynamics is expected to obey is given by the fraction of FG modules that are in non-cued trees, including the special case of isolated modules.

The value of the mean coordination number adopted here, which is biologically reasonable, makes the number of modules that are either isolated or in trees negligibly small. However, the subgraph made of the active modules in the pattern to retrieve has mean coordination number equal to about  $zt_1$ , which is significantly smaller than  $z$ ; the trees of this subgraph, that is, the *activity isles*, may constitute a non-negligible fraction of the pattern. In fact, it can be calculated that the fraction of FG modules that are not in non-cued trees is given by

$$G(\varrho) = 1 - \sum_{n \geq 1} \frac{(1 - \varrho)^n}{n!} (nzt_1)^{n-1} e^{-nzt_1}, \quad (3)$$

where  $\varrho$  is the fraction of the pattern to retrieve that is presented as a cue (the modules activated by the cue are randomly chosen among those in the FG of that pattern). It can be easily shown that  $G(\varrho)$  decreases monotonically as  $t_1$  increases, which means that retrieval performance is better for larger  $t_1$ ; however, there is also a non-trivial upper bound to the value of  $t_1$ , function of  $\tau$  and  $z$ , more difficult to quantify (Fulvi Mari 2000).

In the simulations that follow, the biologically plausible values  $z = 15$  (Pucak et al. 1996, Ichinohe et al. 2012) and  $\tau = 0.1$  will be adopted, given which it can be set  $t_1 = 0.25$  (below the upper bound to correlation). With these values, the population of isolated FG trees altogether accounts for an appreciable fraction of the network. This becomes of some relevance when a small cue is presented; for instance, with  $\varrho = 5\%$ , one has that about  $1 - G(0.05) \simeq 2.5\%$  of the FG of the pattern cannot be retrieved. As an example of Griffiths rare regions (Griffiths 1969), the activity isles would be almost trivial if it was not for the fact that they are not defined by just the architecture of connections, but also, and mainly, by the pattern of activity that is globally reactivated: the location of the rare regions varies across the set of patterns, though their total extent stays about the same if the network is large.

In order to estimate the best retrieval performance achievable in the second and final stage of the cued retrieval task, assume that the network is exactly reproducing a memory pattern. The probability  $q$  for any FG module to be reproducing a feature onto which the association weight is larger than 1, which would allow for the module to remain in stable activity, is (for large  $M$ )

$$q \simeq 1 - e^{-zt_1} - zt_1 e^{-zt_1} \left(1 - \frac{\tau t_1}{F^2}\right)^{P-1} \quad (4)$$

for the nLRSS network, and

$$q \simeq 1 - (1 + zt_1)e^{-zt_1} \quad (5)$$

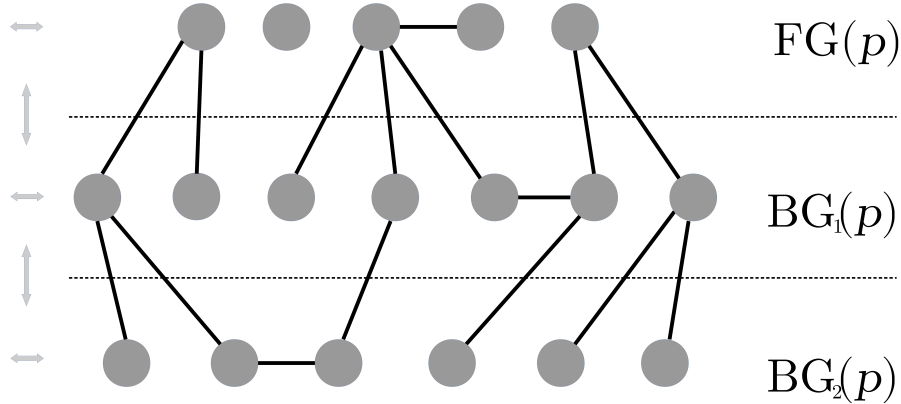


Figure 2: Illustrative diagram of the modular network when pattern  $p$  is perfectly reactivated. From top to bottom: set of active modules, constituting the foreground of pattern  $p$ ; set of quiescent modules of the background that connect directly to foreground modules; set of quiescent background modules that do not connect directly with foreground modules. The shaded arrows on the left show the directions of possible interactions between modules.

for the LRSS network. In fact, one can contemplate special local configurations in which modules cannot be driven to stable retrieval activity and which, therefore, lowers the upper bound a little further, as for similar cases shown by Fulvi Mari (2004); however, such minor contributions turn out to be negligible, especially in comparison to finite-size effects. It may be noticed that  $q$  increases if  $t_1$  increases, which strengthens the idea that pairwise activity correlation is helpful in memory retrieval.

### 3.2 Cued retrieval

At the start of the cued retrieval task, the network is assumed to be quiescent. After a memory pattern to retrieve is chosen, each of the modules that should be active in that pattern is cued by the appropriate feature with probability  $\varrho$  and remains silent otherwise. Immediately after cueing, oscillations begin (with a HR half-wave) as determined by the dynamics defined in Section 2.4. In order to verify time-asymptotic behaviour, the oscillations are let to last enough for the network to reach a stationary regime, although this might be unnecessary in real cognitive tasks. Then, the oscillations stop and robustness is kept at its lower level. The first stage of the process serves the purpose of spreading memory retrieval. The second stage is included for the verification of some dynamical properties, though it may be not relevant to actual cognitive processes; in fact, the quality of retrieval is a little higher in the LR semi-periods of the oscillatory stage than in the static final stage.

In Fig. 2 a very small portion of the network is pictorially reorganised so to illustrate qualitatively the dynamical process. The modules in the FG of the pattern  $p$  to retrieve constitute the set  $FG(p)$  in the top layer. The set  $BG_1(p)$  of modules that do not belong in the pattern but are connected to  $FG(p)$  modules is in the middle layer. The set  $BG_2(p)$  of modules that do not belong in the pattern and are not connected to  $FG(p)$  modules is in the bottom layer. The construction could go on iteratively, though with the values of  $z$  and  $\tau$  adopted here only a tiny fraction of the modules do not belong in any of the layers shown. The arrows on the left indicate the flow of possible spread of activity; as connections are reciprocal, modules

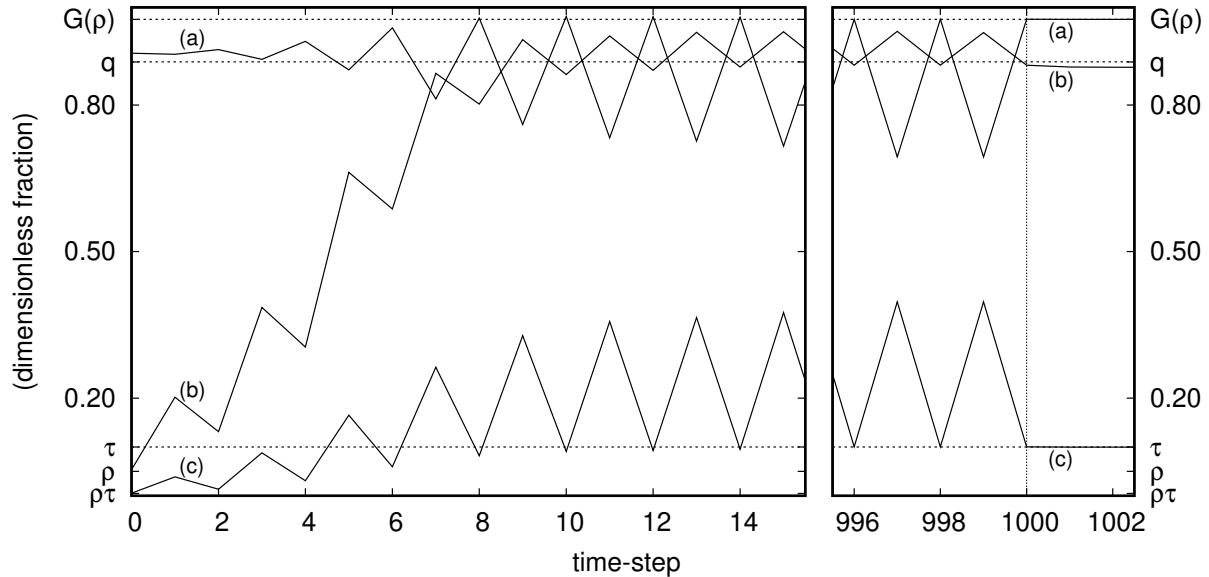


Figure 3: Cued retrieval process: Output from a typical simulation, with  $P = 4000$ ,  $F = 300$ ,  $\tau = 0.1$ ,  $t_1 = 0.25$ ,  $\rho = 5\%$ ,  $M = 25,000$ . The dashed lines represent the predicted values of, from top to bottom, the maximum achievable retrieval quality  $G(\rho)$  during the first stage, the maximum achievable retrieval quality  $q$  during the second stage, and the average activity level  $\tau$  of the pattern to retrieve. Continuous lines: (a) Fraction of modules in the respective correct states (quiescence or active feature); (b) Fraction of  $FG(p)$  modules reproducing the respective correct features; (c) Fraction of active modules. The oscillatory process stops at time=1000.

in a layer can affect modules in the same layer as well as modules in any adjacent layer. At the beginning, the flow is in the downwards direction, but immediately afterwards the reciprocity of connections will allow for activity in a layer to help retrieval spread in any adjacent layer too.

Figure 3 shows the output of a typical numerical simulation of a cued retrieval task in the nLRSS network (the outputs for the LRSS network are qualitatively identical, with insignificant numerical differences). The network has  $M = 25,000$  modules and the fraction of the pattern to retrieve presented as a cue is  $\rho = 5\%$  ( $P = 4000$ ,  $F = 300$ ,  $\tau = 0.1$ ,  $t_1 = 0.25$ ; the values of (b) and (c) at the first peak are well predicted by the expressions A.6 and A.7). The overlaps of the current activity pattern with the other memory patterns are all very small and are not shown as they would just crowd against the zero-ordinate axis. Wrong activation also takes place, as the large peaks of activity in the HR half-waves indicate, but does not spread extensively; at LR, it contributes to global activity by one order of magnitude less than correct activation and does not have significant overlap with any stored pattern.

It may be noticed that it only takes about 5 oscillation periods to achieve maximum retrieval; assuming speculatively that the oscillations are related to brain waves in the gamma range, with a frequency of, say, 50 Hz, the time needed for maximum memory recall is about 100ms, which seems plausible enough and would fit within a semi-period of a 5Hz theta rhythm, the latter having been often hypothesised by other authors as a ‘clock’ for some cognitive processes.

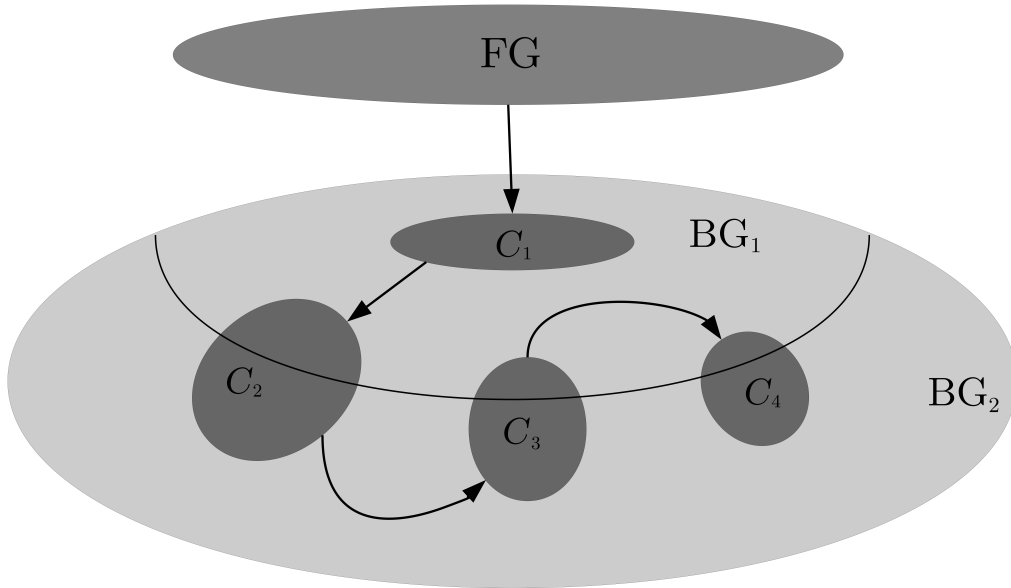


Figure 4: Venn diagram illustrating the possible spread of stable incorrect activity. The darker grey areas  $C_1$ ,  $C_2$ ,  $C_3$ , and  $C_4$ , belonging in the background of the reactivated pattern, represent stable incorrect activity during successive low-robustness half-waves. The set  $BG_1$  comprises the BG modules that are directly connected with FG modules, while the modules of  $BG_2$  connect with modules in  $BG_1$  but not in FG.

### 3.3 Storage capacity

The Venn diagram in Fig. 4 illustrates qualitatively the dynamics of the network in the simulations that were run to estimate the critical storage-load  $P_c$  of the network. At the top is the set of FG modules, all active in the correct respective features by initial condition; this choice was made because it provides an upper bound, as the likelihood of wrong activity spreading is higher when more modules are active. The BG modules that do not belong in  $BG_1 \cup BG_2$  are very few and, hence, are here neglected. At the initial step, the FG modules activate  $BG_1$  modules, some of which, namely  $C_1$ , remain active in the following LR half-wave. Similarly,  $C_1$  modules then produce stable incorrect activity in  $C_2$ , which contains other  $BG_1$  modules as well as some  $BG_2$  modules. Because of recurrent connectivity,  $C_2$  activates other modules both in  $BG_1$  and  $BG_2$ . Activity spread continues in the same manner until a stationary state is reached. Below the critical load, the active sets besides FG are very small, while above it they include most of the network, reproducing features that are altogether not coherent with any stored pattern and bringing the mean activity to much larger values than a correct retrieval state would.

Figure 5 shows the main small subgraphs of relevance in the dynamical spread of activity, which should be considered in isolation for the sake of the following description. Fully connected triplets of modules (3-cliques) are present in negligible number and the corresponding cases are therefore ignored.

Figure 5a shows the case in which one BG module is connected to one only FG module. Module **B** is likely to be activated by module **A** during the HR half-wave. In the LRSS

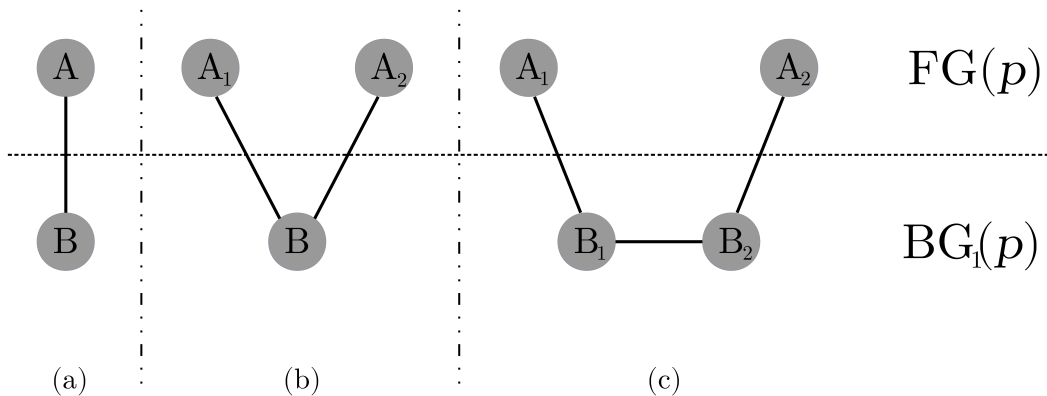


Figure 5: Small subgraphs of special relevance in the qualitative and quantitative analyses of activity spreading.

network, the association weight onto the feature reactivated in **B** cannot be larger than 1 and, therefore, in the following (LR) half-wave, module **B** will become quiescent. In the nLRSS network, module **B** will instead stay stable if there is an association weight larger than 1 onto the reactivated feature.

Figure 5b shows the case in which one BG module is connected to two FG modules. If LRSS is present, activity induced in module **B** can only survive the LR semi-period if the feature it is reproducing is compatible with both the features reproduced respectively by modules **A**<sub>1</sub> and **A**<sub>2</sub>. In the nLRSS network, it would be also sufficient that the association weight from either of the two FG modules onto the feature in **B** be larger than 1.

Figure 5c shows the case in which two BG modules are connected to each other and each to a different FG module. If the respective features they retrieve are compatible with each other, then both **B**<sub>1</sub> and **B**<sub>2</sub> will stay stable in the following LR half-wave because there is a compound association weight larger than 1 onto each of the features they respectively reproduce. This holds for both the LRSS and the nLRSS network; in the nLRSS network, there is the additional possibility that any feature in the BG modules be kept stable by multiple association with the respective FG neighbour.

The three main cases described above suggest that the nLRSS network is more prone to spread of incorrect activity, as there are more possibilities for incorrect activation. Consequently, the storage capacity should be expected to be smaller than in the LRSS network.

The numerical study consisted of several batches of simulations on several realisations of the underlying random graph.<sup>1</sup> For each graph, a large set of memory patterns was created. Every simulation batch was composed of several trials, each organised as follows: the network was loaded with a set of memory patterns below the critical value; one of these pattern was then reactivated as initial condition (equivalent to a memory cue with  $\varrho = 1$ ); one simulation was run; at the end of the run a predefined number of new memory patterns were added; another simulation was then run; such sequence was repeated until several consecutive runs had showed that the load was above critical storage; then, all memory patterns were replaced

<sup>1</sup>Simulation numbers are not specified because they varied through the study depending on the magnitude of fluctuations. Whenever possible, it was chosen to keep running simulations until the sample standard deviation became stationary. The pseudo-random number generator was adapted from routine *run2.c* of Press et al. (2007).

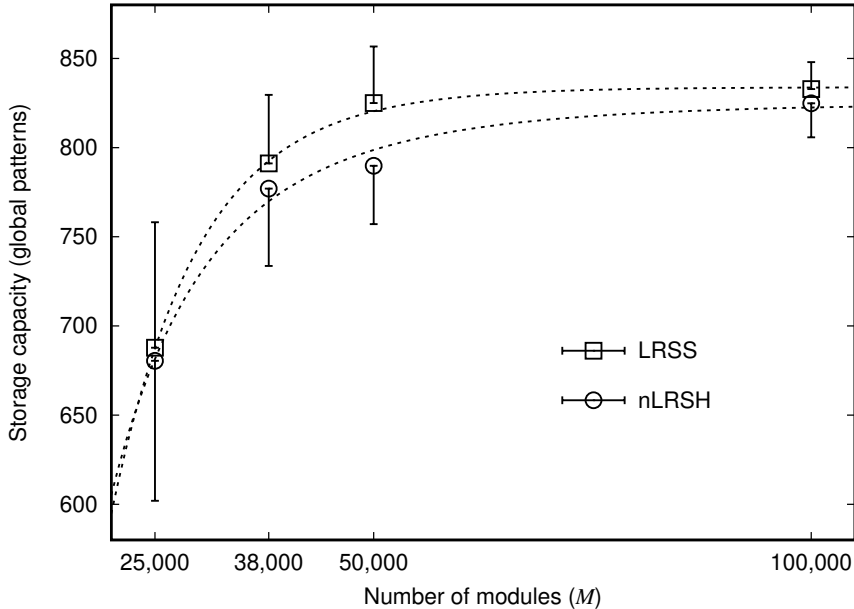


Figure 6: Storage capacity of the modular network as a function of the number  $M$  of modules, the number of features per module being constant ( $F = 100$ ). The segment ending in each data point is as long as the sample standard deviation (to avoid graphics overlap, it is shown only above or below the corresponding point).

and a new trial was started. In any trial, while the number of stored patterns increases towards its critical value, wrong activation gets larger during the HR steps, but it is almost entirely silenced in the LR steps. Extensive spread of stable wrong activity happens suddenly upon storage load reaching the critical value, which makes it easy to measure it, within the limitations due to discretisation; however, such critical number depends significantly on the specific set of patterns that is stored because of finite-size effects, which made it necessary to run a considerable number of simulations with different memory sets in order to achieve a reliable estimate.

Eventually, mean and sample standard deviation of the critical values were calculated. One large set of batches was run on graphs of different sizes while keeping the number of features constant ( $F = 100$ ), the respective critical storage-loads being plotted in Fig. 6; it may be noticed that the standard deviation is proportionally smaller for larger  $M$ , which supports the idea that very large networks will behave almost identically (self-averaging). A second large set of batches was run with different numbers of local features while the size of the graphs was kept constant ( $M = 25,000$ ), the respective critical storage-loads being plotted in Fig 7.

Figure 6 presents a crossover between the two capacity curves at a value of  $M$  below those simulated. It is possible that at smaller network sizes higher order corrections for finite-size effects be required; the crossover, anyway, disappears for more realistic values of  $F$  (e.g.,  $F \geq 1000$ ).

The demand on computer RAM scales approximately as  $MF^2$ , making it unfeasible to simulate the larger networks using the larger numbers of features. A heuristic analysis (Appendix A) guided the search for a functional form of the critical storage-load that agree with both the plots  $(F, P_c)$  and  $(M, P_c)$ . The numerical values of three of the four undetermined parameters

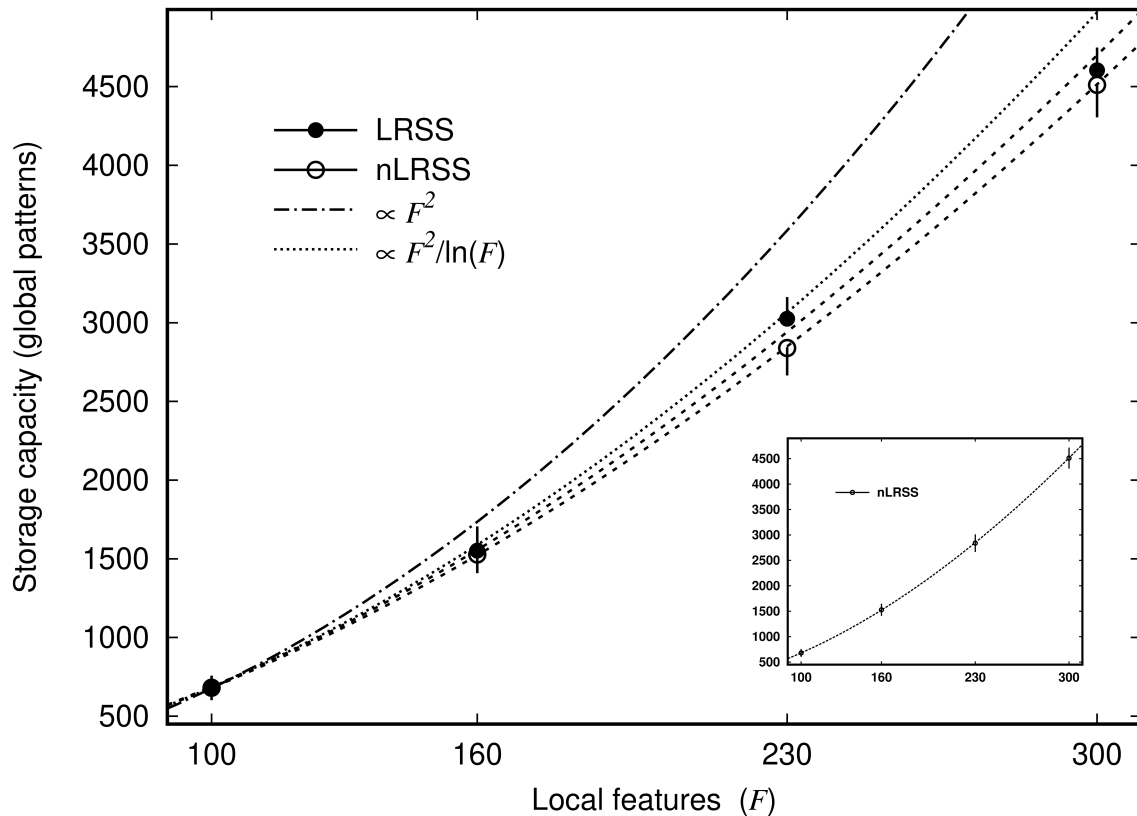


Figure 7: Storage capacity of the modular network as a function of the number  $F$  of features stored in each module, the number of modules being constant ( $M = 25,000$ ). The data points as well as their respective best-fit curves are shown for the LRSS network and for the nLRSS network. The segment ending in each data point is as long as the sample s.d. (to avoid graphics overlap, it is shown only above or below the corresponding point). The curve for a purely quadratic function as well as its correction by a logarithmic denominator are also shown for comparison, both fitted to the two almost coincident data-points for  $F = 100$ . For clarity, the inset re-presents the data points and best-fit curve for the nLRSS network alone.

were estimated by best-fit of the  $(M, P_c)$  data-plot (Fig. 6,  $F \equiv 100$ ), which was derived from a richer data-set<sup>2</sup>. Finally, the value of the remaining parameter was obtained from the  $(F, P_c)$  data-plot (Fig. 7). This procedure led eventually to

$$\begin{cases} P_c \simeq a h(F, M) \frac{F^2}{F^{h(F, M)} - 1} \\ h(F, M) \doteq \beta (\ln F)^{\frac{1+2\mu}{4}} e^{-\nu M^{2(2-\mu)/5}}, \end{cases} \quad (6)$$

where:  $\mu \simeq 0.00$ ,  $a \simeq 0.384$ ,  $\beta \simeq 1.5$ ,  $\nu \simeq 0.001$  in the LRSS network, and  $\mu \simeq 1.00$ ,  $a \simeq 0.380$ ,  $\beta \simeq 6.0$ ,  $\nu \simeq 0.095$  in the nLRSS network. The parameters  $a, \beta, \nu$  depend on the network parameters  $z, \tau, t_1$ , though likely in different ways for the two types of network; regrettably, a numerical study of such dependencies was prohibitive in terms of computational resources. The values of  $\mu$ , however, seem more likely to reflect the combinatorial dissimilarity in the dynamics, though one cannot disregard the fact that the simulation data have significant uncertainties.

<sup>2</sup>As the standard deviation is smaller for larger  $M$  and is due to inherent finite-size effects, it was chosen to use a simple minimisation of sum of square errors in order to avoid underweighting the mean values at lower  $M$ .

It can be noticed straightaway that, for large  $M$ , one has

$$P_c \propto \frac{F^2}{\ln(F)}. \quad (7)$$

For a nLRSS network with  $M = 25,000$  and  $F = 20,000$ , both fairly realistic sizes, Eq. (6) gives  $P_c \sim 10^7$ , which seems plausible. It may also be observed that the average number of features in any module that are associated to any given feature in any adjacent module through a set of stored patterns is

$$\left[ 1 - \left( 1 - \frac{t_1}{F} \right)^{\frac{\tau P}{F}} \right] F, \quad (8)$$

whose value with a storage load just below capacity is about 12.5, which appears to confirm that local ambiguity of associations, consequence of feature-sharing, is indeed present and relevant. As an aside, it may be noticed that, for  $F = 20,000$ , the storage capacity of a network where finite-size effects are no longer relevant ( $M > 100,000$ ) would be predicted by Eq. (6) to be about 10 times that of a network with  $M = 15,000$  (extrapolations to lower values of  $M$  are likely unreliable).

## 4 Discussion

### 4.1 Experimental background

The first general model of a modular organisation of the neocortex was probably the one proposed by Braitenberg (1978). The author based his idea mainly on observations about cytoarchitectonic properties: (1) the pyramidal neurons seem to constitute the computational ‘skeleton’ of the cortex, with the other types of neurons mainly playing a supporting role, (2) the targets of short and, respectively, long range axonal projections are mostly in different layers of the cortical sheet, hinting at some degree of differentiation between local and global processing, and (3) the number of long-range (inter-areal) projections seem far too small to support the theory of an approximately homogeneous architecture. He suggested that the neurons of the cortex are grouped so to form a large number of assemblies: recurrent connectivity inside any assembly is dense, while connections between assemblies are sparse but still enough for the assemblies to work as a whole. This anatomy-based hypothesis is in fact compatible with the then already available evidence of columnar structures and functional modularity (Mountcastle 1957, Hubel & Wiesel 1977). Later, further support for functional modularity, importantly including local reverberation, arrived (Fuster & Jervey 1982, Miyashita 1988, Miyashita & Chang 1988), as did more detailed connectivity studies (Goldman-Rakic 1988, Tommerdahl et al. 1993, Pucak et al. 1996, Ichinohe et al. 2012). Because of experimental constraints, the observed cortical patches in each experiment are few and quite limited in size; therefore, long-range projections are likely undercounted, thus leading to connectivity statistics that might be significantly biased towards a greater dependence of connection probability on distance, some indication of this possibility being apparent, for instance, in the data analysis of Ichinohe et al. (2012). Convincing evidence of large scale recurrent processing in Primates also appeared (Hasegawa et al. 1998, Tomita et al. 1999, Naya et al. 2001, Takeuchi et al. 2011, Hirabayashi et al. 2013, Takeda et al. 2015, Tamura et al. 2017), which showed emphatically that recurrent memory processing is not limited to local assemblies and involves long-range interactions

between plausibly a large number of them, with laminar functional differentiation also being evident. Notwithstanding the correspondence between functional and anatomical modules being debated (Jones 2000, Rakic 2007, Herculano-Houzel et al. 2008, Kaas 2012), it is quite clear that functional columns are geometrically close to be ‘columns’ in only some cortical areas, while being more stripey in others (Pucak et al. 1996). It may be speculated that functional modules derive from coalescence of the phylogenetic mini- or micro-columns, that are known to appear during embryonal development of the cortex.

## 4.2 Theoretical background

The model of O’Kane & Treves (1992) implemented the modular organisation proposed by Braitenberg (1978) quite faithfully. Each module is a Hebbian associative network of the kind studied previously by Treves (1990) as a more biologically-realistic development of earlier models by other authors (Little 1974, Hopfield 1982, Amit et al. 1985, Tsodyks & Feigel’man 1988). Highly dense recurrent connectivity allows each module to store a large number of local features, while the long-range projections from any neuron of any module are distributed randomly across the neurons of the other modules. If, adhering to anatomical data (Braitenberg & Schüz 1991), the number of intramodular afferents per neuron is made similar to that of extramodular ones, the long-range connectivity results to be much more dilute than the local one and, hence, any memory pattern may be considered as made of a specific combination of local features. By employing machinery from equilibrium statistical mechanics in order to study the existence and stability of global memory retrieval states, O’Kane & Treves (1992) found that the landscape of (metastable) network states was largely occupied by ‘memory-glass’, a phase in which modules reproduce respective features locally correct but globally incoherent, so that the network as a whole is, so to speak, in a meaningless state. The global retrieval states are only slightly more robust to noise than memory glass, thus requiring a very fine tuning of noise level that led the authors to question the biological plausibility of a theory of the neocortex as a large complex of interacting autoassociators.

It was later shown (Fulvi Mari & Treves 1998, Fulvi Mari 2000) that including the almost obvious requirement that memory patterns be more realistically sparse, so that only a small fraction of modules are involved in any pattern instead of all of them, only improves the network ability marginally. Making the axonal projections from any module be distributed across a relatively small number of the other modules instead of (statistically) across all of them does also not lead to improvement. However, if the requirement is further added that the activities of any connected pair of modules be correlated across the set of learned patterns, then the proper retrieval states gain a large advantage in robustness with respect to the memory-glass states.

A number of questions remained open, of course. Among them, one was about the retrieval dynamics: the study was addressing the existence of metastable states, but not if and how they may have been reached with biologically realistic dynamics and initial conditions. Another was the estimate of the storage capacity of a multimodular autoassociator: indeed, the signal-to-noise analysis by Fulvi Mari & Treves (1998) was local and could not take into account large-scale cooperative and combinatorial effects.

The first work to address the dynamics of biologically-realistic modular autoassociators was probably the one by Renart et al. (1999). The authors used a firing-rate neuron model to study a network made of three modules, with reciprocal Hebbian synapses between one module and the other two, in the idea that the central module could model a cortical area

at a higher level in the information processing hierarchy than the others. They found that the network can work in several regimes: depending mainly on the value of the parameter that tunes the relative strength of intermodular and intramodular neuronal interactions, the modules can behave with different degree of independence and the retrieval activity can spread more or less easily between them. Their model is capable of reproducing qualitatively well known misperception phenomena due to contradictory inputs from two modalities. However, limiting the network to just three modules, while making it more amenable to an analytical approach and yielding enlightening results, also limited the scope their conclusions could have on networks of several recurrently connected modules.

The dynamics of the spread of neuronal activity through a network of many modules was studied by Fulvi Mari (2004), mainly concerning cued memory retrieval. It was shown that the spread of incorrect activity caused by the local ambiguity of associations (pairwise featural associations are not univocal), which would lead to a meaningless patchwork of pieces from many memory patterns alike memory glass, is mostly prevented if local attractor robustness to noise undergoes periodical oscillations, with a modular dynamics accordingly defined. Differently from the present work, the requirement that any active feature be able to stand destabilising noise was that it has at least two supporting neighbours, having not included, as a first approximation, the role of multiple pairwise association weights. While the laws of the dynamics were defined ad hoc, they turned out to be very compatible with the behaviour of the network of Renart et al. (1999).

In Fulvi Mari (2004), stability of local feature activity is estimated by neuronal signal-to-noise analysis, after which the modular network is treated at a coarse-grained level of multi-state dynamical units, with explicit inhibition being within the intramodular neuronal network only. Having chosen to work directly with modules as multi-state units, Treves (2005) adapted the statistical-mechanical model of Potts neural network to study properties of multimodular autoassociators. He extended the results previously obtained by Kanter (1988) in order to analytically estimate the storage capacity of the modular model at equilibrium, and, after having endowed the modules with a form of adaptation that weakens in time the global attractor in which the network stays, studied by numerical simulations the possibility for the network to travel indefinitely through the set of learned patterns. The synaptic ‘weights’, as in Kanter (1988), are in fact matrices and are allowed to induce both excitation and inhibition of specific features as a consequence of being a generalisation of the covariance rule of Hopfield (1982), in marked contrast with the model presented here, wherein feature-specific intermodular inhibition is not allowed. Whichever of the two contrasting assumptions will result to be more realistic, it is noteworthy that the functional dependence of storage capacity on number of local features is, in the large-network limit, the same for the two models. The precision in the calculation of the storage capacity in Treves (2005), however, comes at the price of bypassing the problems of local ambiguity of associations and of memory glass because of a stochastic dynamics that does not account for robust persistence of local reverberations.

Other models of multimodular networks have subsequently been proposed, though a (brief) comparison will only be made with some of the closest ones. Meli & Lansner (2013) studied an attractor network in which minicolumns are grouped into hypercolumns and connectivity is patchy. They found that it is possible to include representation sparseness and synaptic pruning in their model to make it more realistic without compromising storage capacity, which remains plausibly large; however, only one feature is there associated to each unit, while synaptic pruning does not work as a homeostatic mechanism. With a view at representing concept categorisation, Dubreuil & Brunel (2016) used binary synaptic weights and sparse distribution

of patterns of activity across assemblies of binary neurons to reproduce semantic relations, achieving plausible storage capacity and ability to complete autoassociative tasks (pattern correction or completion) both in individual modules and in the network as a whole. A semantic correlational structure arises in their model as a consequence of how pattern representations are distributed over subsets of modules, conspicuous differences with the present work being though that their architectural intermodular connections are determined by the learning process and that patterns do not share features. Boboeva et al. (2018) made a Potts neural network learn sets of memory patterns with an explicit hierarchical organisation that departs from the simple tree-branching and is compatible with the correlational structure in a data-set of nouns, which in terms of storage capacity only costs a minor reduction. While all these models present characteristics that are to a large extent compatible with, or complementary to, those presented here, the considerable conceptual and mathematical differences in a priori statistics of the memory patterns or modular dynamics make a much deeper comparison difficult.

### 4.3 Summary and conclusions

The dynamics of the network was defined in such a way as to hinder the activation of features that do not belong in the pattern to retrieve according to a memory cue but that may be elicited by correctly activated adjacent modules due to local ambiguity of association. To this end, the robustness of local attractors was made oscillatory, so that any feature in any given module would survive a low-robustness step only if it had support of at least two associations, thus leveraging on combinatorial unlikelihood.

While no attempt was made to justify the existence of the oscillatory mechanism on experimental evidence, there is no shortage of results that lend themselves to educated conjectures in support of the hypothesis, such as modulation of attractor robustness to noise (Durstewitz et al. 2000, Brunel & Wang 2001) and long-range synchronised oscillations (Gray et al. 1989, Wang 2010). A speculative relation with known cortical rhythms yielded a plausible time-scale for the memory retrieval process.

Cued retrieval is achieved with high quality, almost saturating two upper bounds that were analytically estimated: the first bound is relevant during the oscillatory stage and is mostly due to activity isles, which may reflect inability to retrieve small fragments of memory in real cognitive tasks; the second bound is mainly relevant in the final, static stage and is due to the statistical properties of the underlying graph and patterns of activation. Pairwise correlation of activation, which may have semantic significance, plays a worthwhile role in both stages: the quality of retrieval increases if activity correlation between adjacent modules is increased.

Extensive numerical simulations and a heuristic mathematical analysis were carried out to quantify the storage capacity of the network as a function of the number  $F$  of features per module and of the number  $M$  of modules. In fact, finite-size effects are evident if  $M$  is of orders of magnitude that are quite realistic and, therefore, it is meaningful to take them into account. The analytical formula contains few undetermined parameters whose numerical values were estimated from simulation data, resulting in a good fit with the data plots. The fitted curves also appear to confirm that local ambiguity of association is not a negligible phenomenon, as extrapolation to realistically large values of  $F$  shows that multiple pairwise associations can be numerous. In the asymptotic approximation of large  $M$ , the critical storage-load becomes  $P_c \propto F^2/\ln(F)$ , functionally identical to that found in the analytical derivation for extensive Potts neural networks at ‘thermodynamic’ equilibrium (Treves 2005); this suggests that the functional form of the dependence of the storage capacity on  $F$  in large networks is

fundamentally of combinatorial origin. Specifics of, for instance, synaptic weight representation, code sparseness and connectivity are expected to only affect the values of three of the four undetermined parameters, in a way that is not yet analytically explicit in the mathematics of the present model.

The actual storage of all the local features and their associations through a set of memory patterns allowed for investigating the effect of homeostatic synaptic scaling on storage capacity and retrieval abilities. It has been speculated since the results of very early mathematical models of autoassociative memory that some process should exist that could normalise, maybe during sleep, the synaptic weights of a Hebbian network in order to keep it in a working window (Crick & Mitchison 1983). It was also shown in a modular network dynamical model that some mechanism is required to normalise the synaptic weights within each module: because intramodular synaptic-weight increments are of the same sign much more often than those between neurons of different modules, intramodular signals may exceed the extramodular input to the point that multimodular cooperation loses relevance (Fulvi Mari 2004). Experimental evidence shows that synaptic homeostasis does take place (Delvendahl & Müller 2019, Turrigiano 2008, Tononi & Cirelli 2014), although it is not known whether a presumably much more complex associative functional scaling of long-range synapses exist. In the present model, the effects of long-range synaptic scaling are found to only yield a minor increase of storage capacity and to be unimportant during memory retrieval. It seems therefore unlikely that the potential advantage of long-range-coordinated synaptic scaling could constitute enough of an evolutionary drive to lead to the appearance of as a complex mechanism as it would require.

#### 4.4 Research outlook

The presented work largely achieved its objectives, as the dynamics adopted is biologically realistic, wrong activation is mostly suppressed, the quality of retrieval is close to the ideal upper-bound, and the storage capacity is realistically large and compatible with that found in similar models by other approaches. The next step in order of importance should probably be to make the model more realistic by allowing for some wrong activity to randomly survive the destabilising half-wave but not enough to cause robust spread of further wrong activity. Preliminary results suggest that this objective may be fairly easily achieved by introducing global inhibition whose intensity is a monotonic, nonlinear function of the number of active modules. Such modification is compatible with known neuromodulatory mechanisms acting on the neocortex as well as metacognitive theories (since at least the work by Koriat (1993)). Neuronal signal-to-noise analysis showed (Fulvi Mari 2004) that active modules should have higher mean firing-rates than quiescent ones, which can be instrumental to regulating activation by inhibitory feedback loop. The preliminary results also indicate that the centralised inhibitory control may provide the network with the ability to correct errors present in memory cues. However, assuming that the model should just suppress all the fragments from several memory patterns that make up the cue but the largest one of them should not be a foregone conclusion: when and how the network function switches between pattern completion, error correction and segmentation, likely under the influence of neuromodulators, is still very much an open question. Similarly, the separation between learning and retrieval stages in association cortex is also a difficult issue, more than, for instance, in the hippocampal memory system, for semantic learning relies on the extraction of salient information across episodes.

It should be emphasised that the connections between modules in the present model are not

determined by learning, but, rather, learning is thought to adapt to a pre-existing architecture. It is assumed that features that statistically co-occur more often than chance tend to be stored in adjacent modules, rather than edges between modules being determined by learning, the latter seeming not very plausible for white-matter connections. This in itself may already have semantic relevance. Furthermore, it may be conjectured that, while long-range axonal bundles between modules may be at least in part built randomly, the eventual quenched variability of number of neighbours across modules underlie a spontaneous emergence of levels of semantic hierarchy. Indeed, a different number of neighbours may lead to a different degree of semantic value because the features of a module that has more neighbours are subject to larger associative support or to more, different driving inputs. The dynamical approach of the present work seems to be suited to investigating such possibility.

The model is not very amenable to mathematical analysis. Some of the problems of probabilistic combinatorics it presents are non-trivial and possibly of some interest in themselves. Nevertheless, enough progress is conceivably not beyond reach to provide better insight into the dependence of performance on some experimentally measurable quantities and, therefore, endow the model with superior explanatory and predictive power.

## Appendix

### A Probabilistic-combinatorial heuristics for storage capacity

A summary of the reasoning and partial analysis that yielded the formula for storage capacity in Eqs. (6) is here reported. More details will be included in a dedicated, more mathematical paper.

Because of the activity-structure correlation in Eqs. (1), the subgraphs of, respectively, FG and BG modules have mean coordination numbers that differ from  $z$ . By means of Bayesian calculus, for large  $M$  one obtains that the probability for FG modules to be adjacent is

$$\mathbb{P}(\mathbf{A}_1 \leftrightarrow \mathbf{A}_2 | \mathbf{A}_1, \mathbf{A}_2 \in \text{FG}) \simeq \frac{zt_1}{\tau M}, \quad (\text{A.1})$$

for BG modules it is

$$\mathbb{P}(\mathbf{B}_1 \leftrightarrow \mathbf{B}_2 | \mathbf{B}_1, \mathbf{B}_2 \in \text{BG}) \simeq \frac{1-t_0}{1-\tau} \frac{z}{M}, \quad (\text{A.2})$$

which is also valid for  $\text{BG}_1$  modules because the events of being in BG and being adjacent to FG are independent, and for two modules in respectively FG and BG it is

$$\mathbb{P}(\mathbf{B} \leftrightarrow \mathbf{A} | \mathbf{A} \in \text{FG}, \mathbf{B} \in \text{BG}) \simeq \frac{zt_0}{\tau M}. \quad (\text{A.3})$$

One also has that, for large  $M$ ,

$$\mathbb{E}|\text{BG}_1| \simeq (1-\tau)(1-e^{-zt_0})M, \quad (\text{A.4})$$

and

$$\mathbb{E}|\text{BG}_2| \simeq (1-\tau)e^{-zt_0} \left[ 1 - e^{-(1-t_0)z(1-e^{-zt_0})} \right] M, \quad (\text{A.5})$$

the statistical fluctuations being of relative order  $1/\sqrt{M}$ . The same calculations can also be carried out for sets of higher orders; however, inserting the values of the parameters of the networks, it results that at most a few modules do not belong in  $\text{FG} \cup \text{BG}_1 \cup \text{BG}_2$ , which union is therefore the only set of modules taken into consideration.

For large  $M$ , the modules that are correctly active at the first peak of oscillation, which include the cued modules as well as uncued FG modules that are activated by network dynamics, account for a fraction of the network about equal to

$$\tau \varrho + \tau (1 - \varrho) (1 - e^{-\varrho z t_1}), \quad (\text{A.6})$$

while the modules that are driven to incorrect active features, which belong in  $\text{BG}_1$ , account for a fraction of the network about equal to

$$(1 - \tau) \left[ 1 - e^{-\varrho z t_0} \exp \left\{ \varrho z t_0 \left( 1 - \frac{t_1}{F} \right)^{\tau P} \right\} \right], \quad (\text{A.7})$$

that also takes into account the possibility for any  $\text{BG}_1$  module to have several FG neighbours. The sum of the two expressions above gives the fraction of active modules at the first HR peak. These values agree very well with those from the simulations (but for minor statistical fluctuations), which provides a first check on the validity of the assumptions in the network of the chosen size. A finite fraction of the modules so activated will stay stable in the following LR semi-period.

In order to estimate the network storage capacity, the main local configurations to be considered are the small subgraphs in Fig. 5. For the following part, it is convenient to define  $\alpha \equiv \alpha(M, F)$  such that

$$P = \frac{F^2}{\tau t_1 \alpha}. \quad (\text{A.8})$$

Consider first the LRSS network. The case of Fig. 5a, where module **A** reproduces feature  $f$  and module **B** reproduces feature  $g$ , is not relevant because there cannot be an association weight larger than 1 onto feature  $g$ . In the case of Fig. 5b, where modules **A**<sub>1</sub> and **A**<sub>2</sub> reproduce respectively features  $f_1$  and  $f_2$ , the probability for a feature  $g$  to exist in module **B** onto which the compound association weight be larger than 1 is equal to about

$$r_0 \simeq 1 - \left( 1 - \frac{\tau t_1^2}{F^3} \right)^{PF} \simeq 1 - e^{-t_1/\alpha}. \quad (\text{A.9})$$

The case of Fig. 5c is a little more complicated, for pairs of  $\text{BG}_1$  modules cannot be taken in isolation. First, assuming again that modules **A**<sub>1</sub> and **A**<sub>2</sub> reproduce respectively features  $f_1$  and  $f_2$ , one calculates the average number of features of **B**<sub>1</sub> that are associated with  $f_1$ :

$$N(\mathbf{B}_1, f_1) \simeq \left[ 1 - \left( 1 - \frac{\tau t_1}{F^2} \right)^P \right] F \simeq \left( 1 - e^{-1/\alpha} \right) F. \quad (\text{A.10})$$

The same result, obviously, holds for  $N(\mathbf{B}_2, f_2)$ . Then, the probability for any pattern to exist that involve simultaneously one among the  $N(\mathbf{B}_2, f_2)$  features and one among the  $N(\mathbf{B}_2, f_2)$  results to be

$$r_1 \simeq 1 - \left[ 1 - \left( 1 - e^{-1/\alpha} \right)^2 \right]^{F^2/\alpha}. \quad (\text{A.11})$$

With the value of  $z$  adopted in this model, a large majority of the BG modules are in fact in  $\text{BG}_1$ . All such modules already have support by at least one FG module, which implies that their activity is stable if each of them has support from at least another BG module. In terms of the underlying subgraph, one can construct a new random graph with edge probability proportional to  $r_1 z/M$ ; as the number of pairs in BG is proportional to  $M^2$ , one has that, in order to hamper spread of incorrect activity, it must be  $r_1 < n/M$  for some finite  $n$ . This implies that, for any fixed  $M$ ,  $\alpha$  must diverge in the  $F \rightarrow \infty$  limit, which would also make  $r_0$  vanishingly small.

In the nLRSS network, the case of Fig. 5a becomes important. Calling  $f$  the feature reproduced by the FG module  $\mathbf{A}$  and  $g$  the generic feature in  $\mathbf{B}$ , define

$$X_g \doteq \left| \left\{ \text{pattern } p \in [P] \mid g \leftrightarrow f \text{ in } p \right\} \right|, \quad (\text{A.12})$$

and

$$X \doteq \max_{g \in [F]} X_g. \quad (\text{A.13})$$

The probability for  $\mathbf{A}$  to elicit stable incorrect activity in  $\mathbf{B}$  is, for large  $F$ ,

$$r_2 \doteq \mathbb{P}(X \geq 2) \simeq 1 - \left[ e^{-1/\alpha} \left( 1 + \frac{1}{\alpha} \right) \right]^F. \quad (\text{A.14})$$

With a reasoning analogous to the one of the previous case, one has that it must be  $r_2 < m/M$  for some finite  $m$ , implying that, for any fixed  $M$ ,  $\alpha$  must diverge in the  $F \rightarrow \infty$  limit.

In the nLRSS network of Fig. 3,  $r_0$ ,  $r_1$ , and  $r_2$  are of similar magnitude, suggesting that all the three small subgraph play a role and that indeed the multiple pairwise featural associations ( $r_2$ ) are relevant to the dynamics, including, importantly, the spread of incorrect activity. Using these values, the number of BG modules driven into incorrect stable activity in the first oscillation was estimated well within the correct order of magnitude (the fraction of wrongly active modules is not plotted but was present in the numerical outputs of the simulations).

The formulae for, respectively,  $r_1$  and  $r_2$  suggest that, for any arbitrarily large but fixed  $M$ ,  $\alpha$  should diverge faster than  $F$ . Therefore, it was tried the function

$$\alpha \propto F^\xi + c, \quad (\text{A.15})$$

where  $c$  may be constant or weakly dependent on  $F$  and  $M$ . Functions in which  $\xi$  depended on  $M$  but not on  $F$  could not produce acceptably good fits simultaneously to the data in Fig. 6 and in Fig. 7. Hence,  $\xi$  was also allowed to depend on  $F$ , looking first for dependence on powers of  $\ln(F)$ , as suggested by the equations above. In order to conjecture a functional form for the dependence on  $M$ , it was observed that, because the local dynamics in the network depends on the average number of neighbours per module and because such number stays constant in the limit  $M \rightarrow \infty$ , it should be

$$\lim_{M \rightarrow \infty} \alpha = \varphi(F) \in \mathbb{R}. \quad (\text{A.16})$$

If  $\xi$  diverged for  $M \rightarrow \infty$  and fixed  $F$ , the storage capacity would vanish in such limit. Therefore, the limit should be a constant. From the simulations it appears that the constant in question is zero (Fig. 6) and also that  $\varphi(F)$  cannot be constant (Fig. 7). Requiring that  $\xi \rightarrow 0$  and  $\alpha \rightarrow \varphi(F)$  for  $M \rightarrow \infty$  leads to

$$\alpha \propto \frac{1}{\xi} \left( F^\xi - 1 \right). \quad (\text{A.17})$$

Best-fit of the data of Fig. 6, shows that  $\xi$  should depend exponentially on  $M$ .

## B Table of main symbols and acronyms

$M$	Number of modules in the network
$F$	Number of features per module
$P$	Number of memory patterns stored
$z$	Mean coordination number of the graph
$\tau$	Probability for any module to be active in any pattern
$\tau t_1$	Probability for any adjacent pair of modules to be both active
$(1 - \tau) t_0$	Probability for any adjacent pair of modules to be of opposite activity
FG	Foreground of a specified pattern
BG	Background of a specified pattern
LRSS	Presence of long-range synaptic scaling (e.g., LRSS network)
nLRSS	Absence of long-range synaptic scaling
HR	High-robustness, in relation to featural local attractors
LR	Low-robustness, in relation to featural local attractors
$\varrho$	Fraction of a memory pattern used as a cue
$P_c$	Critical storage-capacity
$a, \beta$	Undetermined parameters, to estimate by best-fit

## References

- Amit, D. J., Gutfreund, H. & Sompolinsky, H. (1985). Spin-glass models of neural networks, *Phys. Rev. A* **32**: 1007–1018.
- Binder, J. R., Desai, R. H., Graves, W. W. & Conant, L. L. (2009). Where is the semantic system? A critical review and meta-analysis of 120 functional neuroimaging studies, *Cereb. Cortex* **19**: 2767–2796.
- Boboeva, V., Brasselet, R. & Treves, A. (2018). The capacity for correlated semantic memories in the cortex, *Entropy* **20**: 824.
- Bollobás, B. (2001). *Random Graphs*, 2 edn, Cambridge University Press.
- Braitenberg, V. (1978). Cortical architectonics: general and areal, in M. Brazier & H. Petsche (eds), *Architectonics of the Cerebral Cortex*, Raven Press, New York, U.S.A., pp. 443–465.
- Braitenberg, V. & Schüz, A. (1991). *Anatomy of the Cortex: statistics and geometry*, Springer-Verlag, Berlin Heidelberg.
- Brunel, N. & Wang, X.-J. (2001). Effects of neuromodulation in a cortical network model of object working memory dominated by recurrent inhibition, *J. Comput. Neurosci.* **11**: 63–85.
- Crick, F. & Mitchison, G. (1983). The function of dream sleep, *Nature* **304**: 111–114.
- Delvendahl, I. & Müller, M. (2019). [Review] Homeostatic plasticity – a presynaptic perspective, *Curr. Opin. Neurobiol.* **54**: 155–162.
- Dubreuil, A. M. & Brunel, N. (2016). Storing structured sparse memories in a multi-modular cortical network model, *J. Comput. Neurosci.* **40**: 157–175.

- Durstewitz, D., Seamans, J. K. & Sejnowski, T. J. (2000). Dopamine-mediated stabilization of delay-period activity in a network model of prefrontal cortex, *J. Neurophysiol.* **83**: 1733–1750.
- Erdős, P. & Rényi, A. (1960). On the evolution of random graphs, *Publ. Math. Inst. Hungar. Acad. Sci.* **5**: 17–61.
- Fulvi Mari, C. (2000). Random fields and probability distributions with given marginals on randomly correlated systems: a general method and a problem from theoretical neuroscience, *J. Phys. A: Math. Gen.* **33**: 23–38.
- Fulvi Mari, C. (2004). Extremely dilute modular neuronal networks: Neocortical memory retrieval dynamics, *J. Comput. Neurosci.* **17**: 57–79.
- Fulvi Mari, C. & Treves, A. (1998). Modeling neocortical areas with a modular neural network, *BioSystems* **48**: 47–55.
- Fuster, J. M. & Jervey, J. P. (1982). Neuronal firing in the inferotemporal cortex of the monkey in a visual memory task, *J. Neurosci.* **2**: 361–375.
- Gilbert, E. N. (1959). Random graphs, *Ann. Math. Stat.* **30**: 1141–1144.
- Goldman-Rakic, P. S. (1988). Changing concepts of cortical connectivity: parallel distributed cortical networks, in P. Rakic & W. Singer (eds), *Neurobiology of neocortex*, John Wiley, pp. 177–202.
- Gray, C. M., König, P., Engel, A. K. & Singer, W. (1989). Oscillatory responses in cat visual cortex exhibit inter-columnar synchronization which reflects global stimulus properties, *Nature* **338**: 334.
- Griffiths, R. B. (1969). Nonanalytic behavior above the critical point in a random Ising ferromagnet, *Phys. Rev. Lett.* **23**: 17–19.
- Hasegawa, I., Fukushima, T., Ihara, T. & Miyashita, Y. (1998). Callosal window between prefrontal cortices: Cognitive interaction to retrieve long-term memory, *Science* **281**: 814–818.
- Herculano-Houzel, S., Collins, C. E., Wong, P., Kaas, J. H. & Lent, R. (2008). The basic nonuniformity of the cerebral cortex, *Proc. Natl. Acad. Sci. USA* **105**: 12593–12598.
- Hirabayashi, T., Takeuchi, D., Tamura, K. & Miyashita, Y. (2013). Microcircuits for hierarchical elaboration of object coding across primate temporal areas, *Science* **341**: 191–195.
- Hopfield, J. J. (1982). Neural networks and physical systems with emergent collective computational abilities, *Proc. Natl. Acad. Sci. USA* **79**: 2554–2558.
- Hubel, D. H. & Wiesel, T. N. (1977). Functional architecture of macaque monkey visual cortex, *Proc. R. Soc. London B* **198**: 1–59.
- Ichinohe, N., Borra, E. & Rockland, K. (2012). Distinct feedforward and intrinsic neurons in posterior inferotemporal cortex revealed by in vivo connection imaging, *Sci. Rep.* **2**: 934.

- Jones, E. G. (2000). Microcolumns in the cerebral cortex, *Proc. Natl. Acad. Sci. USA* **97**: 5019–5021.
- Kaas, J. H. (2012). Evolution of columns, modules, and domains in the neocortex of primates, *Proc. Natl. Acad. Sci. USA* **109**: 10655–10660.
- Kanter, I. (1988). Potts-glass models of neural networks, *Phys Rev A* **37**: 2739–2742.
- Koriat, A. (1993). How do we know that we know - The accessibility model of the feeling of knowing, *Psychol. Rev.* **100**: 609–639.
- Little, W. A. (1974). The existence of persistent states in the brain, *Math. Biosci.* **19**: 101–120.
- Meli, C. & Lansner, A. (2013). A modular attractor associative memory with patchy connectivity and weight pruning, *Network: Comput. Neural Sys.* **24**: 129–150.
- Miyashita, Y. (1988). Neuronal correlate of visual associative long-term memory in the primate temporal cortex, *Nature* **335**: 817–820.
- Miyashita, Y. & Chang, H. S. (1988). Neuronal correlate of pictorial short-term memory in the primate temporal cortex, *Nature* **331**: 68–70.
- Mountcastle, V. B. (1957). Modality and topographic properties of single neurons of cat somatic sensory cortex, *J. Neurophysiol.* **20**: 408–434.
- Naya, Y., Yoshida, M. & Miyashita, Y. (2001). Backward spreading of memory-retrieval signal in the primate temporal cortex, *Science* **291**: 661–664.
- O’Kane, D. & Treves, A. (1992). Short- and long-range connections in autoassociative memory, *J. Phys. A: Math. Gen.* **25**: 5055–5069.
- Press, W. H., Teukolsky, S. A., Vetterling, W. T. & Flannery, B. P. (2007). *Numerical Recipes: The Art of Scientific Computing*, Cambridge University Press, Cambridge, U. K.
- Pucak, M. L., Levitt, J. B., Lund, J. S. & Lewis, D. A. (1996). Patterns of intrinsic and associational circuitry in monkey prefrontal cortex, *J. Comp. Neurol.* **376**: 614–630.
- Rakic, P. (2007). [Review] The radial edifice of cortical architecture: From neuronal silhouettes to genetic engineering, *Brain Res. Rev.* **55**: 204–219.
- Renart, A., Parga, N. & Rolls, E. T. (1999). Associative memory properties of multiple cortical modules, *Network: Comput. Neural Syst.* **10**: 237–255.
- Takeda, M., Koyano, K. W., Hirabayashi, T., Adachi, Y. & Miyashita, Y. (2015). Top-down regulation of laminar circuit via inter-area signal for successful object memory recall in monkey temporal cortex, *Neuron* **86**: 840–852.
- Takeuchi, D., Hirabayashi, T., Tamura, K. & Miyashita, Y. (2011). Reversal of interlaminar signal between sensory and memory processing in monkey temporal cortex, *Science* **331**: 1443–1447.
- Tamura, K., Takeda, M., Setsuie, R., Tsubota, T., Hirabayashi, T., Miyamoto, K. & Miyashita, Y. (2017). Conversion of object identity to object-general semantic value in the primate temporal cortex, *Science* **357**: 687–692.

- Tomita, H., Ohbayashi, M., Nakahara, K., Hasegawa, I. & Miyashita, Y. (1999). Top-down signal from prefrontal cortex in executive control of memory retrieval, *Nature* **401**: 699–703.
- Tommerdahl, M., Favorov, O., Whitsel, B. L., Nakhle, B. & Gonchar, Y. A. (1993). Mini-columnar activation patterns in cat and monkey S1, *Cerebral Cortex* **3**: 399–411.
- Tononi, G. & Cirelli, C. (2014). [Review] Sleep and the price of plasticity: From synaptic and cellular homeostasis to memory consolidation and integration, *Neuron* **81**: 12–34.
- Treves, A. (1990). Threshold–linear formal neuron in auto–associative nets, *J. Phys. A: Math. Gen.* **23**: 2631–2650.
- Treves, A. (2005). Frontal latching networks: a possible neural basis for infinite recursion, *Cogn. Neuropsych.* **22**: 276–291.
- Tsodyks, M. V. & Feigel'man, M. V. (1988). The enhanced storage capacity in neural networks with low activity level, *Europhys. Lett.* **6**: 101–105.
- Turrigiano, G. G. (2008). [Review] The self-tuning neuron: Synaptic scaling of excitatory synapses, *Cell* **135**: 422–435.
- Wang, X.-J. (2010). [Review] Neurophysiological and computational principles of cortical rhythms in cognition, *Physiol. Rev.* **90**: 1195–1268.

## Conflicts of interest

None.

## Funding

This research did not receive any financial support of any kind.